

# Quasi-Monte Carlo vs Monte Carlo for High-Dimensional Integration on $[0, 1]^d$

Tanner Wagner  
MATH 505: Numerical Analysis  
University of New Mexico

November 30, 2025

## Abstract

This project compares plain Monte Carlo (MC) and quasi-Monte Carlo (QMC) methods based on Sobol sequences for high-dimensional integrals over  $[0, 1]^d$ . This project looks at several smooth test functions with known exact integrals and compares the methods in terms of absolute error, empirical convergence rate, and practical time-to-accuracy for dimensions  $d \in \{5, 10, 15, 20\}$ .

# Contents

<b>1</b>	<b>Introduction</b>	<b>3</b>
<b>2</b>	<b>Mathematical Background and Methods</b>	<b>3</b>
2.1	High-dimensional integration on $[0, 1]^d$ . . . . .	3
2.2	Brief probabilistic background . . . . .	4
2.3	Quadrature rules and Monte Carlo integration . . . . .	6
2.4	Plain Monte Carlo integration . . . . .	6
2.5	Quasi-Monte Carlo with Sobol sequences . . . . .	7
2.6	Error metrics and comparison criteria . . . . .	8
<b>3</b>	<b>Test Integrands and Experimental Setup</b>	<b>9</b>
3.1	Dimensions and general problem statement . . . . .	9
3.2	Test integrands with known exact values . . . . .	9
3.3	Sample sizes and repetitions . . . . .	12
3.4	Error computation . . . . .	13
3.5	Timing measurements . . . . .	13
3.6	Summary of comparison metrics . . . . .	14
<b>4</b>	<b>Numerical Results</b>	<b>14</b>
4.1	Error versus sample size . . . . .	14
4.2	Error versus time (time-to-accuracy) . . . . .	19
<b>5</b>	<b>Discussion and Conclusions</b>	<b>23</b>
5.1	Summary of numerical findings . . . . .	23
5.2	Rates, constants, and effective dimension . . . . .	23
5.3	Practical takeaways . . . . .	24
<b>6</b>	<b>Works Cited</b>	<b>25</b>
<b>A</b>	<b>Python Code and Data Files</b>	<b>25</b>

# 1 Introduction

High-dimensional integrals appear in many applications, including expectations in probability and statistics, option pricing in finance, and posterior averages in Bayesian inference. In these settings one often needs to approximate integrals over a hypercube such as  $[0, 1]^d$ . Classical deterministic quadrature methods (e.g., Gaussian or composite Newton–Cotes rules) are powerful in low dimensions, but their cost grows very rapidly with  $d$  if we use tensor-product constructions. This *curse of dimensionality* quickly makes standard quadrature prohibitively expensive.

Monte Carlo (MC) methods offer a dimension-robust alternative. By viewing an integral as the expectation of a function of a random variable, Monte Carlo approximates the integral by the average of  $N$  random samples. Under mild conditions, the error decays like  $O(N^{-1/2})$ , essentially independent of  $d$  in the exponent, but this convergence is relatively slow. Quasi–Monte Carlo (QMC) methods seek to improve on this by replacing random samples with deterministic low-discrepancy points (such as Sobol sequences) that are more uniformly distributed over  $[0, 1]^d$ . For smooth integrands with suitable structure and low effective dimension, QMC can achieve much smaller errors than MC for the same  $N$ , and heuristically exhibits an  $O(N^{-1})$ -like behavior up to logarithmic factors.

The goal of this project is to compare plain Monte Carlo and Sobol quasi–Monte Carlo for high-dimensional integration on  $[0, 1]^d$ . We focus on three smooth, separable test integrands with known exact values, including a Gaussian-type integrand related to the normal distribution, together with a fourth smooth polynomial integrand that has low effective dimension and is particularly favorable to QMC. For dimensions  $d \in \{5, 10, 15, 20\}$  and a range of sample sizes  $N$ , we measure absolute error, empirical convergence rates, and practical time-to-accuracy for both methods.

The rest of the paper is organized as follows. Section 2 reviews the probabilistic background and formulates MC and QMC as quadrature rules. Section 3 describes the test integrands and experimental setup. Section 4 presents numerical comparisons of MC and QMC, both as functions of the sample size  $N$  and of wall-clock time. Section 5 summarizes the main findings, emphasizing the roles of dimension, effective dimension, and problem-dependent constants, and discusses possible extensions.

## 2 Mathematical Background and Methods

### 2.1 High-dimensional integration on $[0, 1]^d$

We are interested in approximating integrals of the form

$$I(f, d) = \int_{[0,1]^d} f(x) dx, \quad x = (x_1, \dots, x_d) \in [0, 1]^d.$$

Here  $[0, 1]^d$  denotes the  $d$ -dimensional unit cube, i.e., each coordinate  $x_j$  ranges between 0 and 1. When  $d = 1$  this is a single integral over  $[0, 1]$ ; when  $d = 2$  it is a double integral over the unit square; and in general it is a  $d$ -fold integral over the unit cube.

It is often convenient to interpret  $I(f, d)$  as an *average value* of  $f$  over  $[0, 1]^d$ . This viewpoint naturally leads us to a short review of basic probability concepts.

## 2.2 Brief probabilistic background

I'll briefly introduce the notions of random variables, expectation, and the law of large numbers that underlie Monte Carlo integration.

**Random variables and expectation.** A (real-valued) *random variable*  $Y$  is a quantity whose value is not fixed, but instead is determined by some random experiment. For example,  $Y$  could represent the outcome of rolling a die, or the value of a function evaluated at a randomly chosen point.

The *expectation* (or expected value) of  $Y$ , denoted  $\mathbb{E}[Y]$ , is the average value we would obtain if we repeated the experiment many times and averaged the outcomes. In the continuous setting, if  $Y$  has a probability density function  $p(y)$ , then

$$\mathbb{E}[Y] = \int_{-\infty}^{\infty} y p(y) dy.$$

More generally, for any function  $g(Y)$  we define

$$\mathbb{E}[g(Y)] = \int_{-\infty}^{\infty} g(y) p(y) dy.$$

In our setting, we'll consider a random vector

$$X = (X_1, \dots, X_d)$$

that is *uniformly distributed* on  $[0, 1]^d$ . This means that every region of  $[0, 1]^d$  with the same volume is equally likely. The corresponding density  $p(x)$  is constant on  $[0, 1]^d$  and zero outside. In this special case, the expectation of  $f(X)$  is

$$\mathbb{E}[f(X)] = \int_{[0,1]^d} f(x) dx = I(f, d).$$

Thus the integral  $I(f, d)$  we wish to approximate is exactly the expected value of  $f(X)$  when  $X$  is uniformly distributed on  $[0, 1]^d$ .

**Variance and standard deviation.** The *variance* of a random variable  $Y$  is defined by

$$\text{Var}(Y) = \mathbb{E}[(Y - \mathbb{E}[Y])^2],$$

and measures the spread of  $Y$  around its mean. The *standard deviation* is  $\sqrt{\text{Var}(Y)}$  and has the same units as  $Y$ . Intuitively, the standard deviation is a measure of the typical size of the deviation  $Y - \mathbb{E}[Y]$ .

**Law of large numbers (LLN).** Suppose  $Y_1, Y_2, \dots$  are independent copies of the same random variable  $Y$  (we write  $Y_i$  are i.i.d.). Consider the sample average

$$\bar{Y}_N = \frac{1}{N} \sum_{i=1}^N Y_i.$$

The *law of large numbers* states that, under mild assumptions,

$$\bar{Y}_N \rightarrow \mathbb{E}[Y] \quad \text{as } N \rightarrow \infty,$$

i.e., the sample average converges to the expected value. Intuitively, if we take more and more samples, their average stabilizes near the true mean.

In our application, we'll take  $Y_i = f(X_i)$ , where  $X_i$  are random points in  $[0, 1]^d$  chosen independently and uniformly. The law of large numbers then tells us that the average of the values  $f(X_i)$  converges to the integral  $I(f, d)$ .

**Fluctuations and the  $N^{-1/2}$  scaling.** We are not only interested in convergence, but also in *how fast* the sample average approaches its mean. A key quantity is the fluctuation

$$\bar{Y}_N - \mathbb{E}[Y],$$

which measures how far the sample average wanders away from the true mean for a typical sample.

A simple variance calculation already reveals the  $N^{-1/2}$  scaling. If  $\text{Var}(Y) = \sigma^2 < \infty$  and  $Y_i$  are i.i.d., then

$$\text{Var}(\bar{Y}_N) = \text{Var}\left(\frac{1}{N} \sum_{i=1}^N Y_i\right) = \frac{1}{N^2} \sum_{i=1}^N \text{Var}(Y_i) = \frac{1}{N^2} \cdot N\sigma^2 = \frac{\sigma^2}{N}.$$

Therefore the standard deviation of the sample average is

$$\sqrt{\text{Var}(\bar{Y}_N)} = \frac{\sigma}{\sqrt{N}}.$$

Since the standard deviation is a measure of the typical size of  $\bar{Y}_N - \mathbb{E}[Y]$ , we see that

$$|\bar{Y}_N - \mathbb{E}[Y]| \text{ is typically of size } O(N^{-1/2}).$$

**Central limit theorem (CLT).** The *central limit theorem* refines this by describing the shape of the distribution of the error. Under mild conditions,

$$\sqrt{N} (\bar{Y}_N - \mathbb{E}[Y]) \Rightarrow \mathcal{N}(0, \sigma^2),$$

where  $\Rightarrow$  denotes convergence in distribution and  $\mathcal{N}(0, \sigma^2)$  is a normal (Gaussian) distribution with mean zero and variance  $\sigma^2$ . This again shows that the natural scale of the error  $\bar{Y}_N - \mathbb{E}[Y]$  is  $1/\sqrt{N}$ , consistent with the variance calculation above.

In the Monte Carlo setting we will take  $Y_i = f(X_i)$ , so the Monte Carlo error is exactly a sample average minus a mean, and its typical size is of order  $N^{-1/2}$ .

## 2.3 Quadrature rules and Monte Carlo integration

Any numerical integration method can be viewed as replacing the continuous integral by a finite weighted sum of function values. More precisely, a *quadrature rule* with  $N$  points has the form

$$Q_N(f) = \sum_{i=1}^N w_i f(x_i),$$

where  $x_i \in [0, 1]^d$  are the nodes and  $w_i \in \mathbb{R}$  are weights. Classical deterministic quadrature rules (e.g., trapezoidal or Gaussian quadrature in one dimension, and tensor-product versions in low dimensions) correspond to carefully chosen deterministic nodes and weights.

Monte Carlo and quasi-Monte Carlo methods also fit this template, but with different choices of nodes. In particular, Monte Carlo uses *random* nodes, while quasi-Monte Carlo uses *deterministic* nodes that are designed to be evenly spread over the integration domain.

## 2.4 Plain Monte Carlo integration

Plain Monte Carlo (MC) integration applies the ideas from the previous subsection directly. We draw random points

$$X_1, \dots, X_N \sim \text{Unif}([0, 1]^d)$$

independently and identically distributed, and approximate the integral by the sample average

$$\hat{I}_N^{\text{MC}}(f, d) = \frac{1}{N} \sum_{i=1}^N f(X_i).$$

This is a quadrature rule of the form

$$Q_N(f) = \sum_{i=1}^N w_i f(x_i),$$

with random nodes  $x_i = X_i$  and equal weights  $w_i = 1/N$ .

Because  $\mathbb{E}[f(X_i)] = I(f, d)$ , the estimator is unbiased:

$$\mathbb{E}[\widehat{I}_N^{\text{MC}}(f, d)] = I(f, d).$$

Moreover, the law of large numbers implies that

$$\widehat{I}_N^{\text{MC}}(f, d) \rightarrow I(f, d) \quad \text{as } N \rightarrow \infty,$$

so the Monte Carlo approximation converges to the true integral when we take more and more random points.

The variance calculation from the previous subsection can be applied with  $Y_i = f(X_i)$  and  $\bar{Y}_N = \widehat{I}_N^{\text{MC}}(f, d)$ . If  $\text{Var}(f(X)) = \sigma^2 < \infty$ , then

$$\text{Var}(\widehat{I}_N^{\text{MC}}(f, d)) = \frac{\sigma^2}{N},$$

and the standard deviation (a measure of the typical size of the error) is

$$\sqrt{\text{Var}(\widehat{I}_N^{\text{MC}}(f, d))} = \frac{\sigma}{\sqrt{N}}.$$

Thus the Monte Carlo error

$$\widehat{I}_N^{\text{MC}}(f, d) - I(f, d)$$

has typical magnitude of order  $N^{-1/2}$ . In the language of big- $O$  notation, the root mean square error (RMSE) satisfies

$$\sqrt{\mathbb{E}[(\widehat{I}_N^{\text{MC}} - I)^2]} = O(N^{-1/2}),$$

with a constant that depends on the variance of  $f(X)$  and may grow with the dimension  $d$ , but the exponent  $-1/2$  itself does not depend on  $d$ . This  $N^{-1/2}$  scaling is a hallmark of Monte Carlo methods.

## 2.5 Quasi-Monte Carlo with Sobol sequences

Quasi-Monte Carlo (QMC) methods replace the random nodes of Monte Carlo with a deterministic sequence of points that is designed to fill the unit cube  $[0, 1]^d$  as uniformly as possible. Let  $(x_i)_{i \geq 1}$  be a *low-discrepancy sequence* in  $[0, 1]^d$ , such as a Sobol sequence. The corresponding QMC estimator is

$$\widehat{I}_N^{\text{QMC}}(f, d) = \frac{1}{N} \sum_{i=1}^N f(x_i).$$

This again has the quadrature form  $Q_N(f) = \frac{1}{N} \sum f(x_i)$ , but now the nodes  $x_i$  are carefully constructed rather than random.

The key quantity in QMC analysis is the (star) discrepancy  $D^*(x_1, \dots, x_N)$  of the first  $N$  points, which measures how far the empirical distribution of the points deviates from the uniform distribution on  $[0, 1]^d$ . Lower discrepancy means the points are more uniformly spread out.

For functions of bounded variation in the sense of Hardy-Krause, the Koksma-Hlawka inequality states that

$$|\widehat{I}_N^{\text{QMC}}(f, d) - I(f, d)| \leq V_{\text{HK}}(f) D^*(x_1, \dots, x_N),$$

where  $V_{\text{HK}}(f)$  is the (Hardy-Krause) variation of  $f$ . For many low-discrepancy sequences (including Sobol), the discrepancy satisfies

$$D^*(x_1, \dots, x_N) = O\left(\frac{(\log N)^d}{N}\right) \quad \text{as } N \rightarrow \infty.$$

Ignoring the logarithmic factor  $(\log N)^d$ , this suggests that QMC can achieve an error that behaves like  $O(N^{-1})$  for sufficiently smooth integrands with “low effective dimension,” which is asymptotically better than the Monte Carlo rate  $O(N^{-1/2})$ .

In practice, QMC methods often show substantially smaller errors than MC for the same  $N$  on smooth, well-behaved integrands, especially in moderate dimensions. When the dimension is very high or the integrand has significant discontinuities or strong localized features, the advantage of QMC can diminish.

## 2.6 Error metrics and comparison criteria

For any method (MC or QMC) that produces an approximation  $\widehat{I}_N(f, d)$  to the integral  $I(f, d)$ , we define the absolute error

$$E_N(f, d) = |\widehat{I}_N(f, d) - I(f, d)|,$$

where  $I(f, d)$  is the exact integral, known in closed form for our chosen test functions. We will compare MC and QMC using three related criteria:

1. **Error versus sample size:** we will plot  $E_N(f, d)$  versus  $N$  on logarithmic scales and estimate empirical convergence rates by fitting a slope to  $\log_{10}(E_N)$  versus  $\log_{10}(N)$  for each method.
2. **Error versus wall-clock time:** we will record the computation time required to obtain each approximation and compare time-to-accuracy by plotting  $E_N(f, d)$  against wall-clock time.

3. **Variance and stability:** when repeated runs are performed (for Monte Carlo and, optionally, randomized QMC), we will summarize the distribution of errors (for example, via mean and standard deviation) to assess the stability of the estimators.

This framework allows us to quantify both the asymptotic behavior (convergence rates) and the practical performance (time-to-accuracy) of plain Monte Carlo and Sobol quasi-Monte Carlo integration on high-dimensional test problems.

## 3 Test Integrands and Experimental Setup

In this section we describe the specific test problems and experimental parameters used to compare Monte Carlo and quasi-Monte Carlo integration on high-dimensional integrals over  $[0, 1]^d$ .

### 3.1 Dimensions and general problem statement

For each experiment we fix a dimension

$$d \in \{5, 10, 15, 20\},$$

and consider integrals of the form

$$I(f, d) = \int_{[0,1]^d} f(x) dx, \quad x = (x_1, \dots, x_d) \in [0, 1]^d.$$

The goal is to approximate  $I(f, d)$  using both plain Monte Carlo (MC) and Sobol quasi-Monte Carlo (QMC), and to measure the resulting errors and computation times.

### 3.2 Test integrands with known exact values

To evaluate the accuracy of MC and QMC, we choose test functions  $f : [0, 1]^d \rightarrow \mathbb{R}$  for which the integral  $I(f, d)$  can be computed in closed form (possibly involving special functions). This allows us to compute the *true error*  $|\widehat{I}_N(f, d) - I(f, d)|$  for each method and each configuration.

The first three test integrands we use,  $f_A$ ,  $f_B$ , and  $f_C$ , are *separable* in the sense that they factor into a product of one-dimensional functions,

$$f(x) = \prod_{j=1}^d g_j(x_j),$$

so that the  $d$ -dimensional integral reduces to a product of one-dimensional integrals,

$$I(f, d) = \int_{[0,1]^d} f(x) dx = \prod_{j=1}^d \int_0^1 g_j(x_j) dx_j.$$

This structure makes it straightforward to obtain exact values while still providing a variety of behaviors for the numerical methods.

We work with four test integrands in total, denoted  $f_A$ ,  $f_B$ ,  $f_C$ , and  $f_D$ .

**Integrand A (separable exponential).** Our first test integrand is a symmetric exponential:

$$f_A(x) = \exp\left(-\sum_{j=1}^d x_j\right) = \prod_{j=1}^d e^{-x_j}.$$

The exact integral is

$$I(f_A, d) = \int_{[0,1]^d} f_A(x) dx = \prod_{j=1}^d \int_0^1 e^{-x_j} dx_j = \prod_{j=1}^d (1 - e^{-1}) = (1 - e^{-1})^d.$$

This integrand is smooth, bounded, and treats all coordinates symmetrically.

**Integrand B (rational integrand with arctan closed form).** The second test integrand is a smooth rational function. For  $j = 1, \dots, d$  define

$$g_j(x_j) = \frac{1}{1 + jx_j^2},$$

and set

$$f_B(x) = \prod_{j=1}^d g_j(x_j) = \prod_{j=1}^d \frac{1}{1 + jx_j^2}.$$

Each one-dimensional factor has an explicit antiderivative:

$$\int_0^1 \frac{1}{1 + jx_j^2} dx_j = \frac{1}{\sqrt{j}} \arctan(\sqrt{j} x_j) \Big|_{x_j=0}^{x_j=1} = \frac{1}{\sqrt{j}} \arctan(\sqrt{j}),$$

so that

$$I(f_B, d) = \prod_{j=1}^d \frac{1}{\sqrt{j}} \arctan(\sqrt{j}).$$

This integrand is smooth but has a different shape from the exponential example: it is close to 1 near  $x_j = 0$  and decays as  $x_j$  increases, with the rate depending on  $j$ . The dependence on  $j$  introduces a form of anisotropy, since directions corresponding to larger  $j$  are damped more strongly.

**Integrand C (Gaussian-type integrand).** The third test integrand is inspired by the Gaussian (normal) distribution. We define

$$f_C(x) = \exp\left(-\sum_{j=1}^d x_j^2\right) = \prod_{j=1}^d e^{-x_j^2}.$$

The corresponding one-dimensional integral

$$\int_0^1 e^{-x^2} dx$$

does not have an elementary antiderivative, but it is a classical integral that can be expressed in terms of the *error function*, defined by

$$\operatorname{erf}(z) = \frac{2}{\sqrt{\pi}} \int_0^z e^{-t^2} dt.$$

From this definition we obtain

$$\int_0^1 e^{-x^2} dx = \frac{\sqrt{\pi}}{2} \operatorname{erf}(1).$$

Therefore, by separability,

$$I(f_C, d) = \int_{[0,1]^d} f_C(x) dx = \prod_{j=1}^d \int_0^1 e^{-x_j^2} dx_j = \left( \int_0^1 e^{-x^2} dx \right)^d = \left( \frac{\sqrt{\pi}}{2} \operatorname{erf}(1) \right)^d.$$

This integrand is smooth and strongly related to the Gaussian integral that underlies the normal distribution, providing a natural probabilistic connection in our test set.

**Integrand D (low effective dimension).** To include an example that is especially favorable to quasi-Monte Carlo, we define

$$f_D(x) = \left( \frac{1}{5} \sum_{j=1}^5 x_j \right)^2, \quad x \in [0, 1]^d, \quad d \geq 5.$$

This integrand is smooth and depends only on the first five coordinates, so it has low *effective* dimension even when the nominal dimension  $d$  is large. Let  $X_1, \dots, X_5$  be independent  $\text{Unif}(0, 1)$  random variables and set

$$S = X_1 + \dots + X_5.$$

Then

$$I(f_D, d) = \mathbb{E}\left[\left(\frac{S}{5}\right)^2\right] = \frac{1}{25} \mathbb{E}[S^2] = \frac{1}{25} (\text{Var}(S) + (\mathbb{E}S)^2).$$

Since  $\mathbb{E}X_i = \frac{1}{2}$  and  $\text{Var}(X_i) = \frac{1}{12}$ , we have

$$\mathbb{E}S = 5 \cdot \frac{1}{2} = \frac{5}{2}, \quad \text{Var}(S) = 5 \cdot \frac{1}{12} = \frac{5}{12},$$

and hence

$$\mathbb{E}[S^2] = \text{Var}(S) + (\mathbb{E}S)^2 = \frac{5}{12} + \left(\frac{5}{2}\right)^2 = \frac{20}{3}.$$

Therefore

$$I(f_D, d) = \frac{1}{25} \cdot \frac{20}{3} = \frac{4}{15}.$$

Thus for any  $d \geq 5$  we have

$$I(f_D, d) = \frac{4}{15},$$

independent of the nominal dimension  $d$ .

Together,  $f_A$ ,  $f_B$ ,  $f_C$ , and  $f_D$  provide a small but diverse collection of high-dimensional test problems. The first three are smooth and separable but differ in symmetry, anisotropy, and decay behavior, while  $f_D$  is a smooth polynomial with low effective dimension, designed to highlight the setting where quasi-Monte Carlo is particularly effective.

### 3.3 Sample sizes and repetitions

For each integrand  $f \in \{f_A, f_B, f_C, f_D\}$ , each dimension  $d \in \{5, 10, 15, 20\}$ , and each numerical method (MC or QMC), we consider a sequence of sample sizes

$$N \in \{2^7, 2^8, \dots, 2^{15}\} = \{128, 256, 512, \dots, 32768\}.$$

This range allows us to observe the convergence behavior over several orders of magnitude in  $N$ .

For *plain Monte Carlo*, the estimator  $\hat{I}_N^{\text{MC}}(f, d)$  is random, so we perform

$$R = 30$$

independent runs for each choice of  $(f, d, N)$ . This yields an ensemble of errors, from which we can compute statistics such as the mean error and standard deviation.

For *Sobol quasi-Monte Carlo*, the estimator  $\hat{I}_N^{\text{QMC}}(f, d)$  is deterministic once  $f$ ,  $d$ , and  $N$  are fixed, so in the simplest version we perform a single run for each configuration. Our framework also allows for *randomized Sobol sequences* (scrambled QMC), in which case we could again take  $R$  repeated runs to estimate a variance; however, in this project we primarily focus on the deterministic Sobol case.

### 3.4 Error computation

For each method, integrand, dimension, and sample size we obtain an approximation  $\widehat{I}_N(f, d)$  to the exact integral  $I(f, d)$ . The *absolute error* is defined by

$$E_N(f, d) = |\widehat{I}_N(f, d) - I(f, d)|.$$

In the Monte Carlo case, the estimator  $\widehat{I}_N^{\text{MC}}(f, d)$  is random, so repeated runs with different random seeds produce different approximations and hence different errors. For a fixed configuration  $(f, d, N)$  we perform  $R$  independent runs, yielding a collection of error values

$$E_N^{(1)}(f, d), E_N^{(2)}(f, d), \dots, E_N^{(R)}(f, d).$$

It is natural to think of these as  $R$  samples from an underlying random variable “error” at sample size  $N$ .

From these  $R$  samples we compute two basic summary statistics:

- the *sample mean error*

$$\overline{E}_N(f, d) = \frac{1}{R} \sum_{r=1}^R E_N^{(r)}(f, d),$$

which is simply the average of the observed errors and serves as an estimate of the typical error size at that  $N$ ;

- the *sample standard deviation* of the error

$$\text{std}_N(f, d) = \sqrt{\frac{1}{R-1} \sum_{r=1}^R (E_N^{(r)}(f, d) - \overline{E}_N(f, d))^2}.$$

The quantity inside the square root is the *sample variance* with denominator  $R-1$  rather than  $R$ ; this choice (sometimes called the Bessel correction) makes the sample variance an unbiased estimator of the true variance of the error when the  $E_N^{(r)}$  are independent samples. The sample standard deviation  $\text{std}_N(f, d)$  therefore provides an estimate of the typical fluctuation of the Monte Carlo error around its mean.

For deterministic QMC, the estimator  $\widehat{I}_N^{\text{QMC}}(f, d)$  (and hence the error  $E_N(f, d)$ ) is fully determined by  $f$ ,  $d$ , and  $N$ , so we simply report the single absolute error for each configuration.

### 3.5 Timing measurements

In addition to accuracy, we are interested in the practical cost of each method. For each run we measure the wall-clock time required to *generate the sample points* and *evaluate the integrand* on those points. We denote this time by  $T_N(f, d)$ .

By plotting the error  $E_N(f, d)$  against the corresponding time  $T_N(f, d)$ , we obtain *time-to-accuracy* plots that show, for example, which method reaches a target error (e.g.  $10^{-3}$ ) in less time for a given integrand and dimension.

### 3.6 Summary of comparison metrics

Summarizing, for each integrand  $f$ , dimension  $d$ , method (MC or QMC), and sample size  $N$ , we collect:

- absolute errors  $E_N(f, d)$  (and, for MC, averages and standard deviations over repeated runs),
- corresponding wall-clock times  $T_N(f, d)$ .

We will use these data to construct:

1. log–log plots of  $E_N(f, d)$  versus  $N$  to estimate empirical convergence rates for MC and QMC,
2. plots of  $E_N(f, d)$  versus  $T_N(f, d)$  to compare time-to-accuracy,

These diagnostics allow us to evaluate both the asymptotic behavior and the practical performance of plain Monte Carlo and Sobol quasi–Monte Carlo integration on the chosen high-dimensional test problems.

## 4 Numerical Results

In this section we present the numerical comparison between plain Monte Carlo and Sobol quasi–Monte Carlo for the four test integrands  $f_A$ ,  $f_B$ ,  $f_C$ , and  $f_D$  in dimensions  $d \in \{5, 10, 15, 20\}$ . For each configuration  $(f, d)$  we consider sample sizes

$$N \in \{2^7, 2^8, \dots, 2^{15}\} = \{128, 256, \dots, 32768\},$$

perform  $R = 30$  independent runs for Monte Carlo, and use a single Sobol net of size  $N = 2^m$  for QMC (via `random_base2` with  $N = 2^m$ ). We report absolute errors  $E_N(f, d) = |\hat{I}_N(f, d) - I(f, d)|$  and corresponding wall-clock times for each method.

### 4.1 Error versus sample size

Figures 1–6 show representative log–log plots of error versus sample size  $N$  for selected integrands and dimensions. In each plot, the blue curve corresponds to the Monte Carlo mean error over  $R = 30$  runs, and the orange curve corresponds to the single Sobol QMC error.

**Integrands  $f_A$  and  $f_B$  in moderate dimension.** For  $d = 5$ , both  $f_A$  and  $f_B$  display the “textbook” quasi–Monte Carlo behavior. As a representative example, Figure 1 shows the error for  $f_A$  in  $d = 5$ .

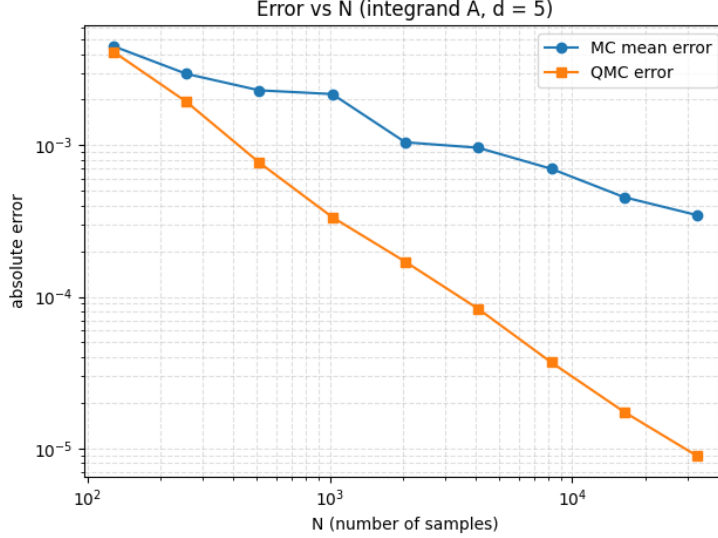


Figure 1: Error versus sample size on a log–log scale for integrand  $f_A$  in dimension  $d = 5$ .

In this case the Sobol QMC curve lies below the MC mean error curve for moderate and large  $N$ . The QMC error decreases roughly linearly in the log–log plot with slope close to  $-1$ , while the MC error decreases more slowly, with a slope closer to  $-1/2$  and noticeably more noise. This is consistent with the theoretical rates  $O(N^{-1})$  for QMC (up to logarithmic factors) and  $O(N^{-1/2})$  for MC for smooth, well-behaved integrands.

A similar picture is observed for  $f_B$  in  $d = 5$  (not shown): QMC again produces smaller errors than MC for large  $N$ , with a nearly straight line of slope close to  $-1$  on the log–log plot.

**Integrands  $f_A$  and  $f_B$  in high dimension.** The situation changes markedly when we increase the dimension to  $d = 20$ . Figures 2 and 3 show the error versus  $N$  for  $f_A$  and  $f_B$  in  $d = 20$ .

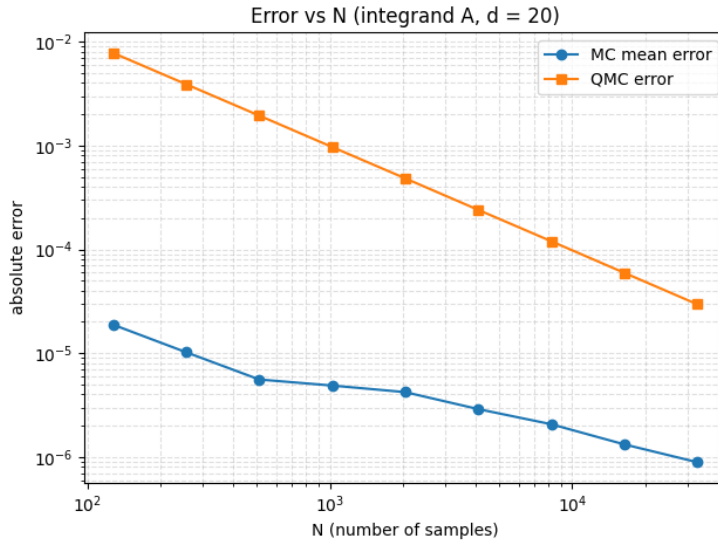


Figure 2: Error versus sample size on a log–log scale for integrand  $f_A$  in dimension  $d = 20$ .

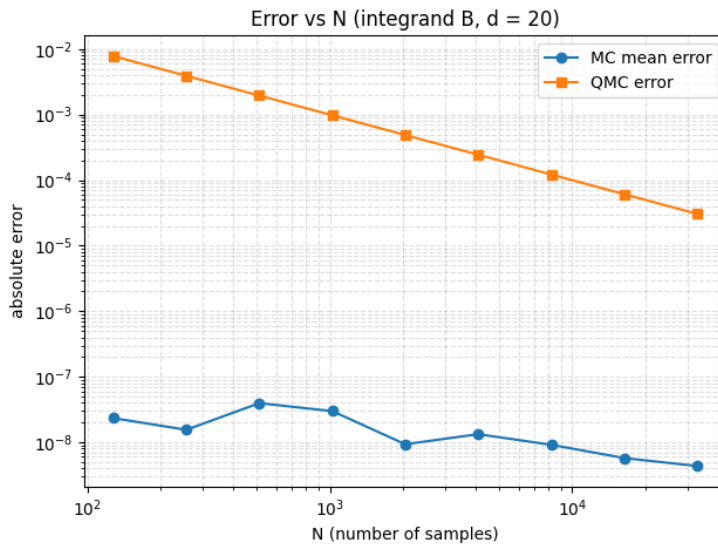


Figure 3: Error versus sample size on a log–log scale for integrand  $f_B$  in dimension  $d = 20$ .

For both  $f_A$  and  $f_B$  in  $d = 20$ , the QMC error still decays roughly like  $O(N^{-1})$  and appears as an almost straight line of slope close to  $-1$  on the log–log plots. However, the QMC errors start at a relatively large value and remain significantly above the MC mean errors throughout the range of  $N$  considered. In contrast, the MC error curves start at much smaller values and decay more slowly, behaving like  $O(N^{-1/2})$ , but nevertheless stay below the corresponding QMC errors for all  $N$  in our experiments.

This illustrates an important point: while QMC enjoys a better *asymptotic* rate, the multiplicative constants in the bounds can be large, especially for high-dimensional integrals

whose exact values (and variances) are extremely small. For  $f_A$  and  $f_B$  in  $d = 20$ , the true integrals are on the order of  $10^{-4}$  and  $10^{-8}$ , respectively. The MC errors inherit this small scale through the variance, whereas the QMC error behaves more like  $C/N$  with a constant  $C$  of order one. Over the practical range of  $N$  used here, MC therefore outperforms QMC.

**Integrand  $f_C$ : pre-asymptotic MC, asymptotic QMC.** For the Gaussian-type integrand  $f_C$ , the behavior in  $d = 20$  lies between the previous two extremes. Figure 4 shows the error versus  $N$  for  $f_C$  in  $d = 20$ .

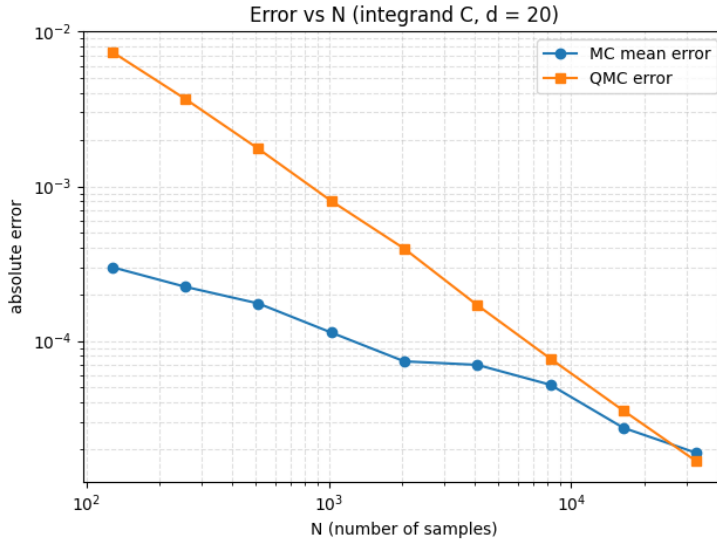


Figure 4: Error versus sample size on a log–log scale for integrand  $f_C$  in dimension  $d = 20$ .

At smaller sample sizes, the MC mean error lies below the QMC error: MC performs better in this “pre-asymptotic” regime. As  $N$  increases, the QMC error decreases more rapidly, with a slope closer to  $-1$  than  $-1/2$ , and eventually the QMC curve meets and slightly undercuts the MC curve at the largest  $N$  values. This example shows a regime where the superior asymptotic rate of QMC becomes visible, but only after a range of  $N$  in which MC gives smaller errors.

**Integrand  $f_D$ : low effective dimension and clear QMC win.** Finally, we consider the low effective-dimension integrand  $f_D$ . Recall that  $f_D$  depends only on the first five coordinates, even when the nominal dimension  $d$  is much larger, and that  $I(f_D, d) = 4/15$  for all  $d \geq 5$ . Figures 5 and 6 show the error versus  $N$  for  $d = 5$  and  $d = 20$ , respectively.

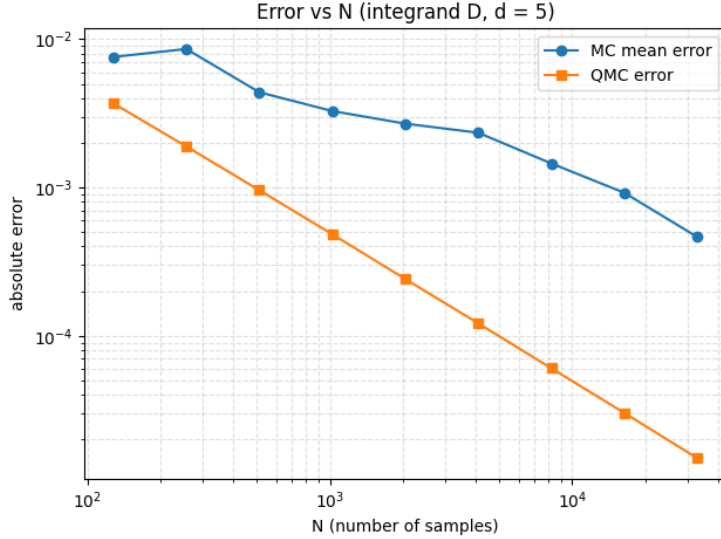


Figure 5: Error versus sample size on a log–log scale for integrand  $f_D$  in dimension  $d = 5$ .

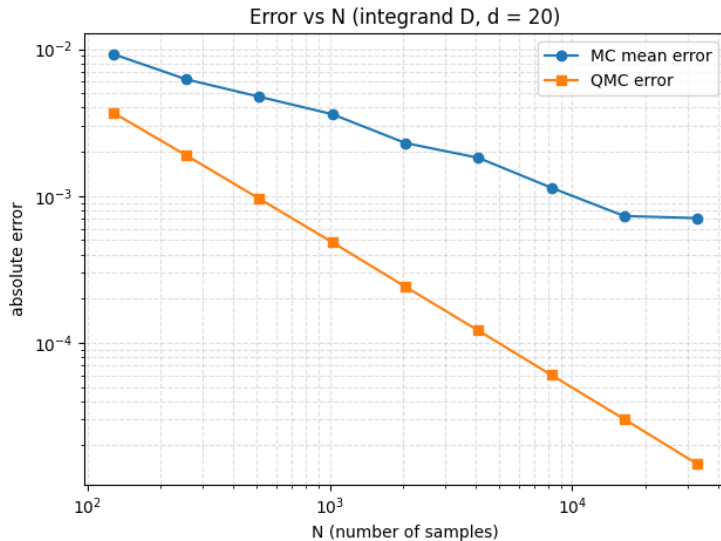


Figure 6: Error versus sample size on a log–log scale for integrand  $f_D$  in dimension  $d = 20$ .

For  $f_D$ , Sobol QMC clearly outperforms MC in both dimensions. The QMC error curve lies below the MC curve for all  $N$  considered and is almost perfectly linear on the log–log scale with a slope close to  $-1$ . The MC mean error exhibits the expected  $O(N^{-1/2})$  decay with more variability and remains roughly an order of magnitude larger than the QMC error at the largest  $N$ . Furthermore, the QMC error curves for  $d = 5$  and  $d = 20$  are very similar, reflecting the fact that the *effective* dimension of the problem is five regardless of the nominal  $d$ . This example confirms the classical theory: when the integrand is smooth and depends primarily on a small number of coordinates, quasi–Monte Carlo can deliver the expected  $O(N^{-1})$ -type behavior and a substantial accuracy advantage over plain Monte Carlo.

## 4.2 Error versus time (time-to-accuracy)

For each of the representative cases above, we also plot the absolute error against the measured wall-clock time. These error-versus-time plots provide a direct view of *time-to-accuracy* for each method.

**Moderate dimension:**  $f_A$  in  $d = 5$ . Figure 7 shows error versus wall-clock time for  $f_A$  in  $d = 5$ .

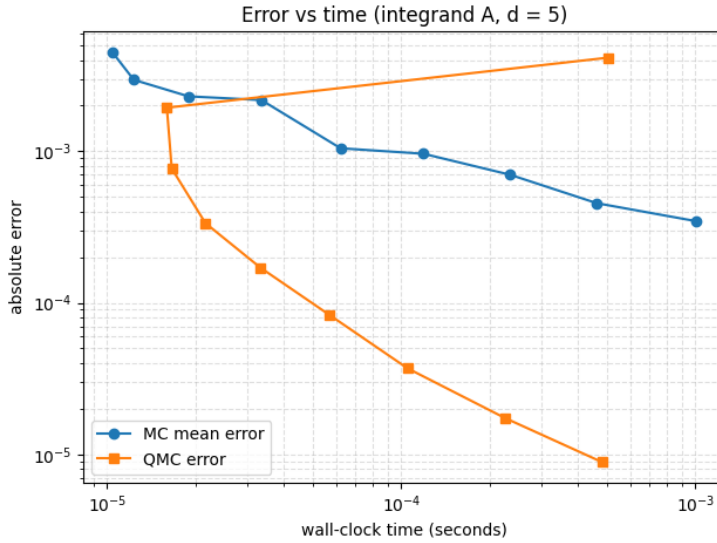


Figure 7: Error versus wall-clock time (log–log) for integrand  $f_A$  in dimension  $d = 5$ .

Because the cost per sample is similar for MC and QMC, the error-versus-time curves closely mirror the error-versus- $N$  behavior: QMC reaches a given target accuracy (for example,  $10^{-3}$ ) in less time than MC, reflecting both its lower error for fixed  $N$  and comparable per-sample cost.

**High dimension:**  $f_A$  and  $f_B$  in  $d = 20$ . Figures 8 and 9 show error versus time for  $f_A$  and  $f_B$  in  $d = 20$ .

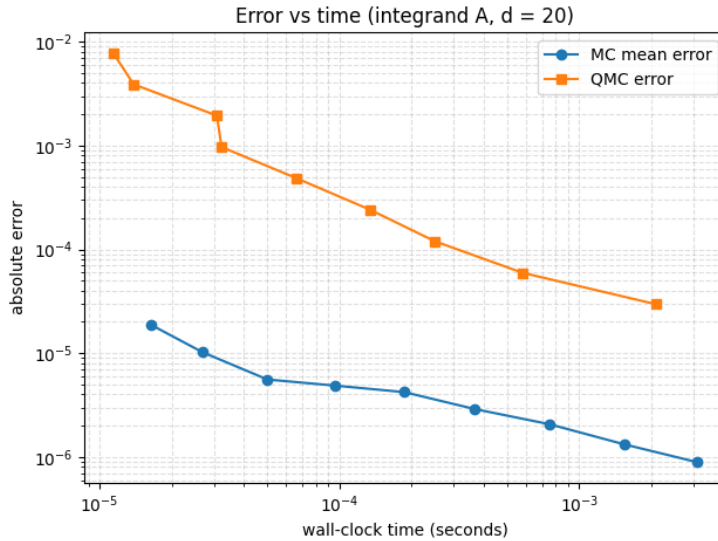


Figure 8: Error versus wall-clock time (log–log) for integrand  $f_A$  in dimension  $d = 20$ .

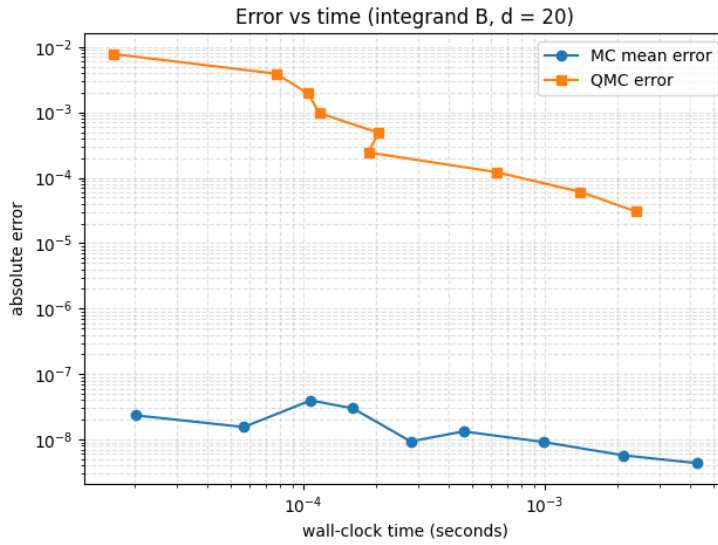


Figure 9: Error versus wall-clock time (log–log) for integrand  $f_B$  in dimension  $d = 20$ .

In both cases, the MC curves lie below the QMC curves for all times in the range studied. This reflects the fact that MC achieves smaller errors than QMC at each sample size  $N$  for these integrands and dimensions. Thus, for  $f_A$  and  $f_B$  in  $d = 20$ , plain Monte Carlo not only has better accuracy for a given  $N$ , but also reaches any fixed error tolerance faster than QMC in terms of wall-clock time.

**Intermediate behavior:  $f_C$  in  $d = 20$ .** For the Gaussian-type integrand  $f_C$  in  $d = 20$ , the time-to-accuracy picture again mirrors the error-versus- $N$  behavior. Figure 10 shows the

error versus wall-clock time.

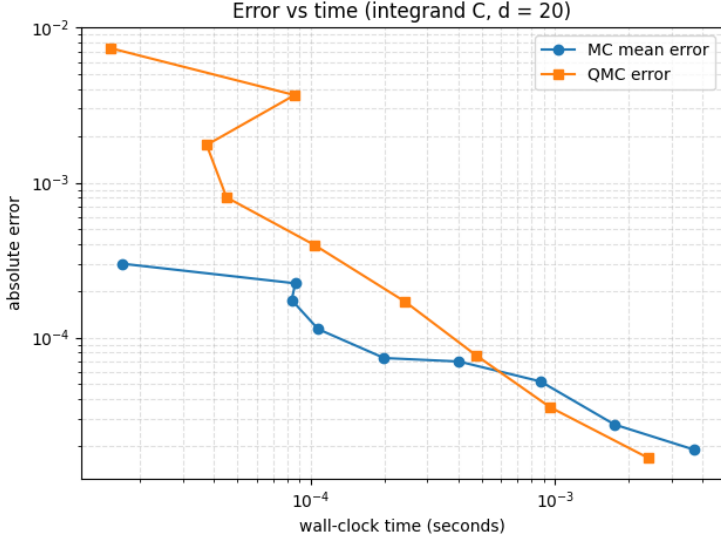


Figure 10: Error versus wall-clock time (log–log) for integrand  $f_C$  in dimension  $d = 20$ .

At small run times (corresponding to small  $N$ ), MC attains smaller errors than QMC. As the run time increases and  $N$  grows, the QMC curve bends downward more steeply and eventually crosses the MC curve at the largest times considered. This is consistent with the interpretation that MC is more effective in a pre-asymptotic regime, while QMC becomes competitive and slightly superior as we move into a regime where its  $O(N^{-1})$ -type behavior starts to dominate.

**Low effective dimension:**  $f_D$  in  $d = 5$  and  $d = 20$ . Finally, for the low effective-dimension integrand  $f_D$ , the error-versus-time plots again underscore the advantage of QMC. Figures 11 and 12 show the error versus time in  $d = 5$  and  $d = 20$ .

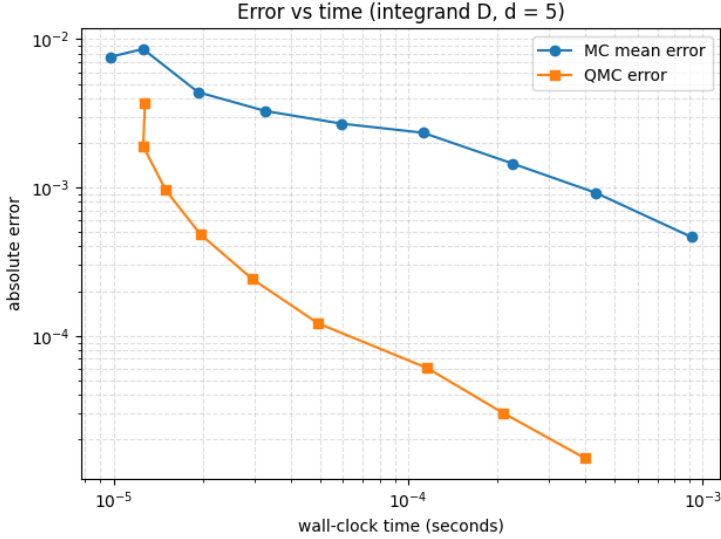


Figure 11: Error versus wall-clock time (log–log) for integrand  $f_D$  in dimension  $d = 5$ .

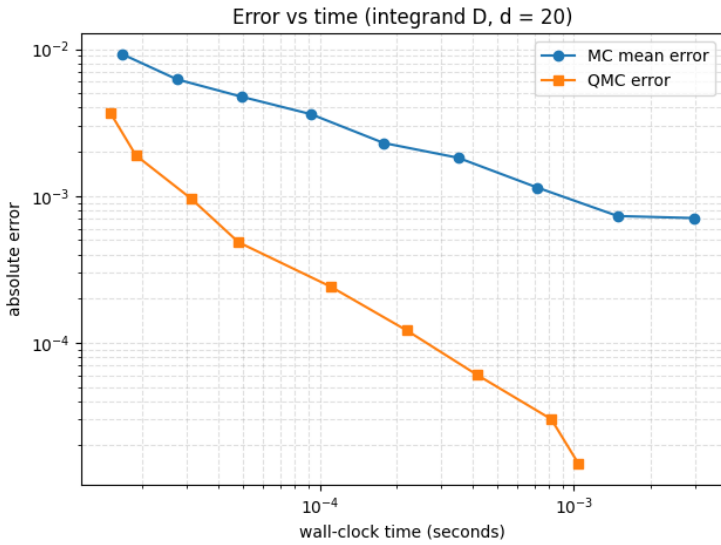


Figure 12: Error versus wall-clock time (log–log) for integrand  $f_D$  in dimension  $d = 20$ .

For both dimensions, the Sobol QMC curve lies well below the MC curve throughout the time range. QMC reaches any given target error much more quickly than MC, and the similarity between the  $d = 5$  and  $d = 20$  curves again highlights that the effective dimension of  $f_D$  is only five.

Overall, the time-to-accuracy plots confirm that the qualitative comparisons observed in the error-versus- $N$  plots translate directly into practical computational efficiency: whenever QMC has smaller error at fixed  $N$ , it also achieves a given tolerance in less wall-clock time, and conversely when MC dominates in error, it is also more efficient in time.

## 5 Discussion and Conclusions

This project compared plain Monte Carlo (MC) and Sobol quasi-Monte Carlo (QMC) for approximating high-dimensional integrals over  $[0, 1]^d$  for a set of smooth test integrands. The numerical experiments were designed to illustrate both the classical theoretical picture— $O(N^{-1/2})$  error for MC versus a potential  $O(N^{-1})$  behavior for QMC—and some of the subtleties that arise in practice, especially in higher dimension.

### 5.1 Summary of numerical findings

Broadly speaking, the experiments support the following observations:

- In moderate dimension ( $d = 5$ ), Sobol QMC behaves very much in line with the standard theory on all three separable integrands  $f_A, f_B, f_C$ . For a fixed number of samples  $N$ , the QMC error is smaller than the Monte Carlo mean error, and the log-log error-versus- $N$  plots for QMC show an almost straight line with slope close to  $-1$ , while the MC curves decay more slowly with slope closer to  $-1/2$  and display more variability.
- In higher dimension ( $d = 20$ ), the picture becomes more nuanced. For  $f_A$  (the separable exponential) and  $f_B$  (the rational integrand), MC actually outperforms QMC over the entire range of sample sizes considered. The QMC error still decreases roughly like  $O(N^{-1})$ , but it starts from a much larger value and remains above the MC mean error for all  $N \leq 32768$ .
- For the Gaussian-type integrand  $f_C$  in  $d = 20$ , MC has smaller errors at small  $N$ , while QMC decays faster and eventually catches up and slightly surpasses MC at the largest  $N$  values. This example shows a transition from a “pre-asymptotic” regime, where MC is more accurate, to a regime where the asymptotic advantage of QMC starts to appear.
- For the low effective-dimension integrand  $f_D$ , Sobol QMC clearly and consistently outperforms MC in both  $d = 5$  and  $d = 20$ . The QMC error curves for  $f_D$  are nearly identical in  $d = 5$  and  $d = 20$ , reflecting the fact that  $f_D$  depends only on the first five coordinates, while the MC errors are larger and exhibit the expected  $O(N^{-1/2})$  decay with more noise.

The error-versus-time plots mirror these conclusions: whenever QMC achieves smaller errors for a given  $N$ , it also reaches a specified target tolerance in less wall-clock time, and conversely in the cases where MC is more accurate.

### 5.2 Rates, constants, and effective dimension

One of the main lessons from these experiments is that the asymptotic rates  $O(N^{-1/2})$  for MC and  $O(N^{-1})$  (up to logarithmic factors) for QMC are only part of the story. The

multiplicative constants and the *effective* dimension of the integrand play a crucial role.

For  $f_A$  and  $f_B$  in  $d = 20$ , the exact integrals  $I(f_A, 20)$  and  $I(f_B, 20)$  are extremely small (on the order of  $10^{-4}$  and  $10^{-8}$ , respectively), and the variance of  $f(X)$  under a uniform random  $X \in [0, 1]^d$  is correspondingly tiny. As a result, the MC error  $\widehat{I}_N^{\text{MC}} - I$  naturally lives on this small scale and is roughly  $\sigma/\sqrt{N}$  with  $\sigma \ll 1$ . In contrast, the QMC error behaves more like  $C/N$  with a constant  $C$  that is effectively of order one. Over the range  $N \leq 32768$ , the advantage of the  $1/N$  rate is not enough to overcome the unfavorable constant, so MC remains more accurate than QMC for these particular integrands and dimensions.

The integrand  $f_C$  illustrates an intermediate situation: the constants are such that MC is better at small  $N$ , but QMC eventually catches up as  $N$  increases and the  $1/N$  decay begins to dominate. In practice, this means that whether QMC is beneficial depends not only on the smoothness of  $f$ , but also on the range of sample sizes one is willing or able to use.

The low effective-dimension example  $f_D$  highlights the setting in which QMC performs in a “textbook” fashion. Although the nominal dimension is as large as  $d = 20$ ,  $f_D$  only depends on the first five coordinates, and the remaining coordinates are irrelevant. In this situation, the Sobol sequence can effectively exploit its low-discrepancy structure in a five-dimensional space, and the error-versus- $N$  curves for  $d = 5$  and  $d = 20$  are nearly identical. MC still converges at the universal  $N^{-1/2}$  rate, but its errors are uniformly larger than those of QMC for all  $N$  in the experiment. This example confirms the theoretical insight that QMC is especially effective when the integrand has low effective dimension or when most of the variation is concentrated in the first few coordinates.

### 5.3 Practical takeaways

From a practical point of view, the experiments suggest the following guidelines:

- For smooth, moderate-dimensional integrals with reasonably sized integrals and variances, Sobol QMC can provide a clear accuracy and efficiency advantage over plain Monte Carlo.
- In very high dimensions, or for integrands whose exact values and variances are extremely small, MC may outperform QMC over the range of sample sizes that are computationally affordable. In these cases, the constants hidden in the  $O(N^{-1})$  and  $O(N^{-1/2})$  notations are important.
- When there is evidence that the integrand has low effective dimension (for example, the integrand mainly depends on a few coordinates or principal components), QMC is particularly attractive and often displays the expected  $N^{-1}$ -type behavior even when the nominal dimension is large.

Overall, the experiments in this project show that quasi-Monte Carlo can indeed achieve the improved convergence behavior suggested by theory in favorable cases, but they also highlight that in high-dimensional, small-variance settings, plain Monte Carlo can be competitive or

even superior over realistic ranges of sample sizes. The choice between MC and QMC (or a combination of both) should therefore be informed by the structure and effective dimension of the particular problem at hand.

## 6 Works Cited

### References

- [1] H. Niederreiter, *Random Number Generation and Quasi–Monte Carlo Methods*, SIAM, 1992.
- [2] C. Lemieux, *Monte Carlo and Quasi–Monte Carlo Sampling*, Springer, 2009.
- [3] A. Quarteroni, R. Sacco, and F. Saleri, *Numerical Mathematics*, 2nd ed., Springer, 2007.
- [4] SciPy Developers, *scipy.stats.qmc.Sobol documentation*, SciPy Reference Guide, <https://docs.scipy.org/doc/scipy/reference/generated/scipy.stats.qmc.Sobol.html>, accessed November 2025.
- [5] A. B. Owen, *Monte Carlo Theory, Methods and Examples*, 2013. Available online at <https://artowen.su.domains/mc/>.

## A Python Code and Data Files

All numerical experiments were implemented in Python using the scripts in the `Code` subdirectory of the project. The main components are:

- `integrands.py`: definitions of the test integrands  $f_A, f_B, f_C, f_D$  and their exact integrals  $I(f, d)$ .
- `mc_qmc.py`: implementations of plain Monte Carlo and Sobol quasi–Monte Carlo estimators on  $[0, 1]^d$ .
- `run_experiments.py`: driver script that runs all experiments over  $f \in \{f_A, f_B, f_C, f_D\}$ ,  $d \in \{5, 10, 15, 20\}$ , and  $N \in \{2^7, \dots, 2^{15}\}$ , and writes the aggregated data to `results_mc_qmc.csv`.
- `plot_results.py`: script that reads `results_mc_qmc.csv` and generates the log–log error versus  $N$  and error versus time plots shown in Section 4.

The file `results_mc_qmc.csv` contains the numerical data used to produce all figures in this report.

A complete copy of the project (Python code, data files, and L<sup>A</sup>T<sub>E</sub>X sources for this report) is available at [https://github.com/yourusername/MATH\\_505\\_Final\\_Project](https://github.com/yourusername/MATH_505_Final_Project).